14. R. D. Chervin, P. A. Pierce, B. W. Connors, *J. Neurophysiol.* **60**, 1695 (1988); R. Miles, R. D. Traub, K. S. Wong, *ibid.*, p. 1481; D. Golomb and Y. Amitai, *ibid.* **78**, 1199 (1997).
15. We note however that smooth waves are possible with on-center synaptic coupling if individual neurons are able to oscillate for some appropriate levels of maintained input (*10*).
16. S. Wagner, M. Castel, H. Gainer, Y. Yarom, *Nature* **387**, 598 (1997); E. Cherubini, J. L. Gaiarsa, Y. Ben-Ari, *Trends Neurosci.* **14**, 515 (1991); K. J. Staley, B. L. Soldo, W. R. Proctor, *Science* **269**, 977 (1995).
17. Using the more complete thalamic model of Golomb *et al.* (*8*), G. Smith and J. Rinzel found (data not shown) footprint-dependent propagation modes. Lurching occurs with on-center footprints. But smooth waves are possible if the effective TC-RE-TC coupling is off-center; for example, if the RE-TC inhibition is off-center while the excitation from TC to RE is narrowly focused on-center.
18. T. Bal, M. von Krosigk, D. A. McCormick, *J. Physiol.* **483**, 665 (1995); U. Kim, M. V. Sanchez-Vives, D. A. McCormick, *Science* **278**, 130 (1997); F.-S. Lo and S. M. Sherman, *Exp. Brain Res.* **100**, 365 (1994).
19. G. Tamas, E. H. Buhl, P. Somogyi, *J. Neurosci.* **17**, 6352 (1997); A. M. Thomson and J. Deuchars, *Trends Neurosci.* **17**, 119 (1994).
20. M. V. Sanchez-Vives and D. A. McCormick [*J. Neurosci.* **17**, 8894 (1997)] report that under normal slice conditions they do not see rebounding in RE cells due to RE-RE $GABA_A$ barrages. D. Ulrich and J. R. Huguenard [*J. Neurophysiol.* **78**, 1748 (1997)] have demonstrated rebounding with injection to the RE cell's soma of dynamic-clamp simulated $GABA_A$ currents.
21. J. Rinzel and G. B. Ermentrout, in *Methods in Neuronal Modeling: From Synapses to Networks*, C. Koch and I. Segev, Eds. (MIT Press, Cambridge, MA, 1989, pp. 135–169).
22. Elements of phase plane analysis for excitable membrane systems can be found in R. FitzHugh, *Biophys. J.* **1**, 445 (1961) and in (*21*). For a two-variable system the nullclines are the two curves in the phase plane along which either variable has zero velocity. In our case, from the differential equations, setting $dV/dt = 0$ gives the V nullcline as $h = [g_L(V - V_L) - I_{app}]/[g_{Ca\text{-}T}m_\infty(V)(V_{Ca} - V)]$ and similarly the h nullcline as $h = h_\infty(V)$. For default parameter values, the steady state for any I_{app} is on the left branch and is therefore stable.
23. Supported by the Alfred P. Sloan Foundation, NSF grants DMS-9203299 and DMS-9626728, NIH grants MH53717-01 and MH 47150, and the W. M. Keck Foundation.

15 August 1997; accepted 15 January 1998

Linkage of Adhesion, Filamentous Growth, and Virulence in *Candida albicans* to a Single Gene, *INT1*

Cheryl A. Gale, Catherine M. Bendel, Mark McClellan, Melinda Hauser, Jeffrey M. Becker, Judith Berman,* Margaret K. Hostetter*

Adhesion and the ability to form filaments are thought to contribute to the pathogenicity of *Candida albicans*, the leading cause of fungal disease in immunocompromised patients. Int1p is a *C. albicans* surface protein with limited similarity to vertebrate integrins. *INT1* expression in *Saccharomyces cerevisiae* was sufficient to direct the adhesion of this normally nonadherent yeast to human epithelial cells. Furthermore, disruption of *INT1* in *C. albicans* suppressed hyphal growth, adhesion to epithelial cells, and virulence in mice. Thus, *INT1* links adhesion, filamentous growth, and pathogenicity in *C. albicans* and Int1p may be an attractive target for the development of antifungal therapies.

Candida albicans is the leading cause of invasive fungal disease in premature infants, diabetics, surgical patients, and hosts with human immunodeficiency virus infection or other immunosuppressed conditions. Despite appropriate therapy, mortality resulting from systemic C. *albicans* infection in immunocompromised patients approaches 30% (*1*). The pathogenesis of C. *albicans* infection is postulated to involve adhesion to host epithelial and endothelial cells and morphologic switching of yeast cells from the ellipsoid blastospore to various filamentous forms: germ tubes, pseudohyphae, and hyphae (*2*).

The C. *albicans* gene *INT1* was originally cloned because of its similarity to vertebrate leukocyte integrins (*3*), adhesins that bind extracellular matrix proteins and induce morphologic changes in response to extracellular signals (*4*). *INT1* expression in the budding yeast S. *cerevisiae* triggers a morphologic switch to filamentous growth (*3*). In C. *albicans*, multiple adhesins mediate attachment to epithelium, endothelium, or platelets (*5–8*). Because laboratory strains of S. *cerevisiae* have few adhesins (*7*), we investigated whether Int1p is present on the cell surface and can function as an adhesin when it is expressed in S. *cerevisiae*.

When intact S. *cerevisiae* cells expressing *INT1* were treated with an impermeant biotinylation reagent, Int1p became biotin-labeled, indicating that at least one portion of Int1p was on the exterior cell surface (Fig. 1A). Nonsurface proteins, such as Rap1p, an abundant nuclear protein, were not biotinylated (Fig. 1A). *Saccharomyces cerevisiae* cells expressing *INT1* (strain YCG101) adhered to monolayers of human cervical epithelial cells (HeLa), whereas S. *cerevisiae* cells carrying vector sequences (YCG102) and YCG101 cells grown in glucose [to repress Int1p expression from the *GAL10* promoter (*9*)] did not adhere to HeLa monolayers (Fig. 1B). Furthermore, adhesion of YCG101 cells to HeLa monolayers was specific for Int1p epitopes: UMN13, a polyclonal antibody recognizing Int1p amino acids 1143 to 1157 [a region predicted to be extracellular (*3*)], inhibited adhesion, whereas nonimmune rabbit immunoglobulin G (IgG) did not (Fig. 1B). Thus, the expression of Int1p alone was sufficient to confer adhesive capacity on S. *cerevisiae*.

INT1 expression induces the growth of highly polarized buds (*3*). To test the possibility that the increased surface area of polarized S. *cerevisiae* cells (Fig. 1C) influences cell adhesion, we performed adhesion assays with a *cdc12-6*^{ts} strain (JKY81-5-1) (*10*) that forms multiple elongated buds at the permissive temperature (*11*) (Fig. 1C). Adhesion of the *cdc12-6*^{ts} strain to HeLa cell monolayers did not differ from that of YCG102 and was significantly less than the adhesion seen upon expression of *INT1* (Fig. 1B), indicating that filamentous morphology alone is not sufficient to explain the increased adhesion of *INT1*-expressing cells.

We next tested the hypothesis that *INT1* is involved in adhesion and filamentous growth in C. *albicans* as well. Both copies of *INT1* were disrupted sequentially in C. *albicans* strain CAI4 (*12*) by means of a *his*G-*CaURA3*-*his*G cassette (*13*) yielding a Ura$^+$ *int1/INT1* heterozygote (CAG1) and a Ura$^+$ *int1/int1* homozygote (CAG3). *INT1-CaURA3* was reintegrated into the genome of a Ura$^-$ *int1/int1* homozygote (CAG4) to yield the *int1/int1* + *INT1* heterozygous reintegrant (CAG5) (*14*), which served as an *int1/int1* + *INT1* Ura$^+$ control to ensure that CAG3 phenotypes could be attributed to disruption of *INT1*.

The specific adhesion of the C. *albicans* *int1/int1* strain (CAG3) to HeLa cells was

C. A. Gale, Department of Pediatrics, University of Minnesota, 420 Delaware Street S.E., Minneapolis, MN 55455, USA, and Department of Plant Biology, University of Minnesota, 220 Biological Sciences Center, St. Paul, MN 55108, USA.
C. M. Bendel, M. McClellan, M. K. Hostetter, Department of Pediatrics, University of Minnesota, 420 Delaware Street S.E., Minneapolis, MN 55455, USA.
M. Hauser and J. M. Becker, Department of Microbiology, University of Tennessee, M409 Walters Life Sciences, Knoxville, TN 37996, USA.
J. Berman, Department of Plant Biology, University of Minnesota, 220 Biological Sciences Center, St. Paul, MN 55108, USA.

*To whom correspondence should be addressed. E-mail: judith@biosci.cbs.umn.edu and hoste001@maroon.tc.umn.edu

reduced by 39% relative to that of the *INT1/INT1* strain (CAF2) (*12*) (Fig. 2A). Preincubation of the *C. albicans INT1/INT1* strain (CAF2) with UMN13 antibodies reduced epithelial adhesion by 40% but did not eliminate it (Fig. 2A). In contrast, preincubation of *S. cerevisiae* expressing *INT1* with UMN13 antibodies blocked virtually all adhesion to HeLa cells (Fig. 1B). These results suggest that although Int1p was the major adhesin expressed in *S. cerevisiae*, other attachment factors in addition to Int1p account for epithelial adhesion in *C. albicans*. The presence of a single copy of *INT1* (CAG1 and CAG5) did not restore wild-type adhesion; however, the single copy of *INT1* in CAG1 and CAG5 was expressed because UMN13 significantly reduced adhesion in these strains by 39% and 28%, respectively (Fig. 2A). As expected, UMN13 did not significantly reduce adhesion in the *int1/int1* strain (CAG3). These results indicate that Int1p is one of a number of adhesins that enable *C. albicans* to attach to epithelial cells, and that the remaining candidal adhesins in the *int1/int1* strain (CAG3) bind HeLa cells by means of

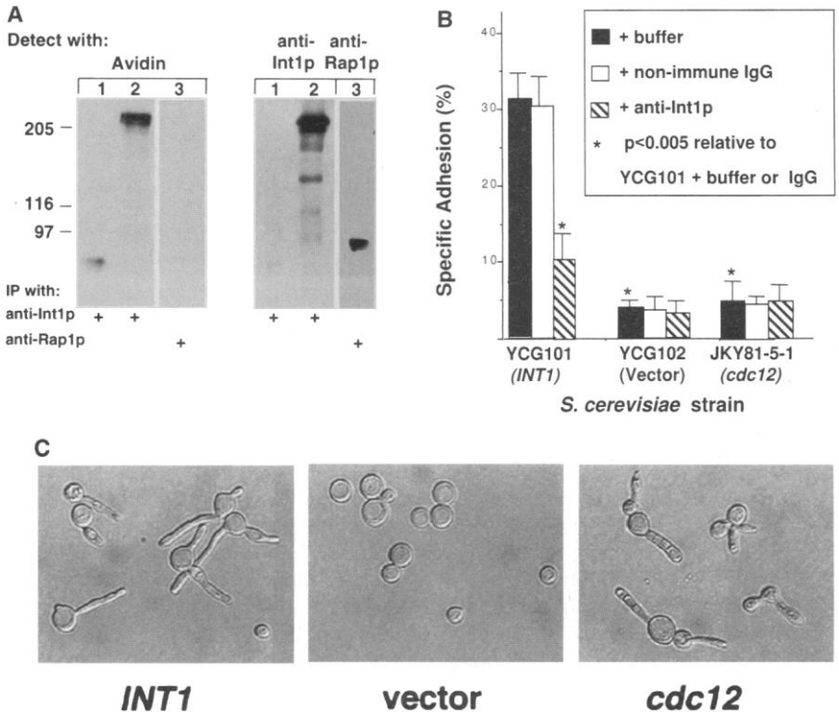

Fig. 1. Int1p is a surface protein that mediates adhesion to human epithelial cells. (**A**) Protein blots of *S. cerevisiae* proteins immunoprecipitated (IP) from cell lysates after labeling of cell surface proteins with biotin (*25*). Left panel, biotinylated proteins detected with HRP-avidin; right panel, proteins detected with the antibodies indicated. Lane 1 of each panel, *S. cerevisiae* expressing vector sequences only; lanes 2 and 3, *S. cerevisiae* expressing *INT1*. Numbers at the left are molecular size markers (in kilodaltons). (**B**) Expression of *INT1* enables *S. cerevisiae* to adhere to human epithelial cells (*26*). Percent specific adhesion was determined for YCG101, *S. cerevisiae* YPH500 (*MATα ura3 lys2 ade2 trp1his3 leu2*) expressing *INT1* under control of the *GAL10* promoter on the plasmid pCG01 (*3*); YCG102, YPH500 transformed with the *GAL10* vector pBM272 (*24*); and JKY81-5-1, *S. cerevisiae cdc12 -6^{ts}* strain (*10*). YCG101 and YCG102 cells were grown to midexponential phase in minimal medium with 2% raffinose and then diluted to an optical density of 0.1 at 600 nm in minimal medium containing 8.7 mM methionine plus 2% galactose for the induction of *INT1*. JKY81-5-1 cells were grown in galactose at 25°C and then shifted to 30°C. (**C**) Morphology of each of the strains tested for adhesive ability. Cells were grown as in (A) and images were obtained with a Leitz Diaplan microscope with differential interference contrast optics, an MTI CCD72 camera, and Scion Image software.

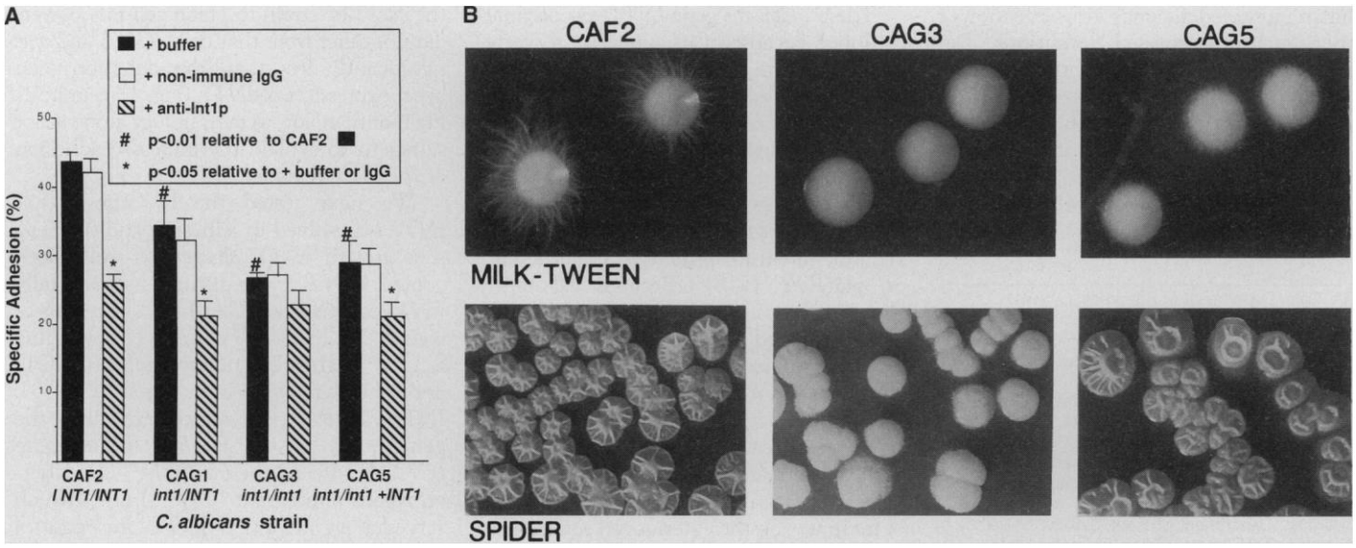

Fig. 2. Disruption of *INT1* in *C. albicans* reduces adhesion to human epithelial cells and filamentous growth. (**A**) Adhesion analysis (*26*) of *INT1/INT1* (CAF2) (*12*), *int1/INT1* (CAG1) (*13*), *int1/int1* (CAG3) (*13*), and *int1/int1* + *INT1* (CAG5) (*14*) strains. (**B**) Hyphal growth of *C. albicans* strains on milk-Tween agar and Spider medium (*27*). Left panels, *INT1/INT1* (CAF2); center panels, *int1/int1* (CAG3); right panels, *int1/int1* + *INT1* (CAG5). Colonies were photographed with a Zeiss Stemi DRC dissecting microscope and a Nikon 35-mm camera.

an epitope or epitopes not recognized by UMN13. Results with the heterozygote strains (CAG1 and CAG5) imply that the gene dosage of *INT1* is important for the full expression of the adhesive phenotype.

The effect of *int1* mutations on the filamentous growth of C. *albicans* strains was monitored with isogenic Ura$^+$ prototrophs on two different media that induce filamentation (Fig. 2B). The *INT1/INT1* strain (CAF2) formed an extensive network of long, branching hyphae that overlay and penetrated milk-Tween agar. On Spider medium, the *INT1/INT1* strain (CAF2) formed wrinkled colonies, an indicator of filamentous growth (*15*). In contrast, the *int1/int1* strain (CAG3) formed smooth-edged colonies with very few filamentous cells emanating from the colony edge on milk-Tween agar and primarily smooth colonies on Spider medium. Reintegration of *INT1* (CAG5) restored the ability of the colonies to produce large numbers of hyphae on milk-Tween agar and to form wrinkled colonies on Spider medium, indicating that *INT1* contributes to the filamentous growth of C. *albicans*.

On both media, filamentous growth of the reintegrant strain (CAG5) (Fig. 2B) and of the *int1/INT1* strain (CAG1) (*9*) was similar, but not identical, to the growth of *INT1/INT1* colonies (CAF2). Similarly, strains heterozygous for the C. *albicans* homologs of *STE7* (*hst7/HST7*), *STE12* (*cph1/CPH1*), and *STE20* (*cst20/CST20*) exhibit intermediate defects in hyphal formation

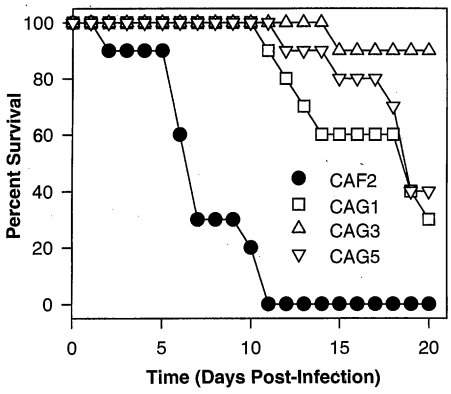

Fig. 3. Disruption of *INT1* in *C. albicans* causes reduced virulence in a mouse model of systemic candidiasis (*28*) (n = 10 mice for each yeast strain). Curves are the compiled results of two replicate experiments (n = 5 mice for each yeast strain for each experiment). Although the first experiment was terminated at day 20, mice in the second experiment were followed until day 30; no additional deaths occurred between day 20 and day 30 in the mice injected with CAG3. The doubling times of all strains, grown in SD minus uracil at 30°C, were 72 ± 6 min, except in the first experiment, where CAG5 had a doubling time of 90 min.

(*16*), suggesting that filamentous growth in C. *albicans* is sensitive to gene dosage.

Despite the altered morphology of the *int1/int1* strain (CAG3) on milk-Tween and Spider media, this strain grew with a phenotype indistinguishable from that of the *INT1/INT1* strain (CAF2) in other liquid and solid media that induce hyphae (*17*), which shows that Int1p is not necessary for the growth of hyphae in C. *albicans*. Rather, the results suggest that Int1p may be a sensor that triggers the morphogenic decision process in response to a subset of environmental conditions. We propose that morphogenesis in C. *albicans* can occur through multiple pathways that include some discrete and some overlapping components. Consistent with this view, mutation of other C. *albicans* genes that are involved in morphogenesis pathways suppress hyphal formation under some, but not all, growth conditions: Mutation of both alleles of the C. *albicans* mitogen-activated protein kinase components *HST7*, *CPH1*, and *CST20* suppresses hyphal growth on solid Spider medium but has no effect on hyphal growth in serum (*16, 18*). In addition, C. *albicans phr1/phr1* strains, which lack a putative surface glycoprotein, affect the morphology of filamentous cells at high but not low pH (*19*).

We tested the virulence of the C. *albicans int1* mutant strains in a mouse model of intravenous infection because both adhesion and hyphal growth are hypothesized to be important for the pathogenicity of C. *albicans*. Again, isogenic *URA3* strains were used because *ura3* strains have reduced virulence (*18, 20*). All of the mice injected with the *INT1/INT1* strain (CAF2) died by day 11 (Fig. 3). In contrast, the *int1/int1* homozygote (CAG3) was much less virulent; 90% of the mice were alive at the end of the experiment (Fig. 3). The virulence of the *int1/int1* strain (CAG3) also was less than that of both heterozygous strains (CAG1 and CAG5) (Fig. 3). These results indicate that Int1p, a protein that functions in both adhesion and filamentous growth, is essential for the virulence of C. *albicans* in this murine model of intravenous infection.

A single copy of *INT1* in the heterozygous C. *albicans* strains CAG1 and CAG5 restored the filamentation phenotype to nearly that of the wild type and restored virulence to an intermediate extent, but did not restore specific adhesion to the same degree. These results could be attributed to a number of possibilities: differences in the threshold amount of Int1p required for the given phenotype, different cell types assayed for each phenotype (yeast forms for adhesion versus filamentous forms for morphogenesis), or differences between the growth or assay conditions used to test each phenotype. The latter two situations may affect the expression of Int1p.

Candida albicans is a highly successful pathogen of immunocompromised hosts, most likely because it has several adhesins and multiple pathways for triggering the morphologic switch to filamentous growth (*16, 18, 19, 21*). Similar to the results with deletion of *INT1*, deletion of *HST7* (*18*) and combined deletion of *CPH1* with *EFG1* (*21*) suppress hyphal formation and virulence in C. *albicans*. Because Int1p is the first C. *albicans* protein shown to be involved in both adhesion and filamentation, it will be interesting to determine how *INT1* regulates, or is regulated by, other pathways of adhesion and morphologic switching in C. *albicans*. Unlike C. *albicans* homologs of S. *cerevisiae* genes involved in pseudohyphal growth (*16, 18, 21*), *INT1* appears to be unique to C. *albicans* (*3*). Moreover, *INT1* induces filaments in strains lacking *STE12* (*3*) and other genes required for pseudohyphal growth (*22*). The S. *cerevisiae* protein Bud4p has sequence similarity to Int1p in the COOH-terminal 300 amino acids; however, Bud4p is not required for Int1p-induced filamentous growth and high-copy *BUD4* expression does not induce filamentous growth (*22*), indicating that Int1p and Bud4p are not functional homologs. Although Int1p has only limited similarity to vertebrate integrins (*3*), it clearly fits the integrin paradigm in its surface localization, its mediation of adhesion, and its ability to influence morphogenesis. Thus, Int1p is a candidal virulence factor that, unlike other reported virulence factors, is involved in both adhesion and morphogenesis. The surface location of Int1p makes it an attractive target for the design of preventive strategies and therapeutic agents.

REFERENCES AND NOTES

1. R. P. Wenzel and M. A. Pfaller, *Infect. Control Hosp. Epidemiol.* **12**, 523 (1991).
2. F. C. Odds, *Candida and Candidosis* (Tindall, London, 1988), pp. 46–47.
3. C. Gale *et al.*, *Proc. Natl. Acad. Sci. U.S.A.* **93**, 357 (1996).
4. E. Ruoslahti and M. D. Pierschbacher, *Science* **238**, 491 (1987); R. Hynes, *Cell* **69**, 11 (1992); E. A. Clark and J. S. Brugge, *Science* **268**, 233 (1995); B. M. Gumbiner, *Cell* **84**, 345 (1996).
5. S. Yan *et al.*, *Infect. Immun.* **64**, 2930 (1996); S. A. Klotz and R. L. Smith, *J. Infect. Dis.* **163**, 604 (1991).
6. P. Maisch and R. A. Calderone, *Infect. Immun.* **27**, 650 (1980).
7. C. M. Bendel and M. K. Hostetter, *J. Clin. Invest.* **92**, 1840 (1993).
8. C. M. Bendel, J. St. Sauver, S. Carlson, M. K. Hostetter, *J. Infect. Dis.* **171**, 1660 (1995).
9. C. Bendel, C. Gale, J. Berman, M. Hostetter, unpublished data.
10. JKY81-5-1 (*MAT***a** *cdc12-6*^{ts} *ade2 cry1 his4 leu2 trp1 ura3 SUP4-3*^{ts}) was provided by J. Konopka (State University of New York at Stony Brook).
11. A. E. M. Adams and J. R. Pringle, *J. Cell Biol.* **98**, 934 (1984); L. H. Hartwell, *Exp. Cell Res.* **69**, 265 (1971).
12. CAI4 (*Caura3/caura3 INT1/INT1*) (*23*) is a Ura$^-$ derivative of CAF2 (*CaURA3/caura3 INT1/INT1*).
13. The *hisG-CaURA3-hisG* Bam HI–Bgl II fragment from

pCUB-6 (*23*) was inserted between the Bcl I sites within the Bgl II–Sal I fragment of *INT1* cloned into the Bam HI–Sal I sites of pUC18 to yield the *int1*-disruption plasmid pCG05. pCG05 digested with Nsp V and Hind III was used to transform the Ura⁻ strain CAI4 (*23*) using a modified spheroplast transformation method [M. B. Kurtz, M. W. Cortelyou, D. R. Kirsch, *Mol. Cell. Biol.* **6**, 142 (1986)]. Ura⁺ transformants were screened by polymerase chain reaction (PCR) and Southern (DNA) blot analysis for integration of the disrupted *INT1* fragment. Southern blot analysis of transformant CAG1 confirmed that a single *hisG-CaURA3-hisG* cassette had integrated into the *INT1* locus. A Ura⁻ segregant (CAG2) was selected on 5-fluoroorotic acid (5-FOA); PCR and Southern blot analysis confirmed that CAG2 had lost *CaURA3* by recombination between the tandem *hisG* repeats. CAG2 was used in an identical round of transformation and 5-FOA selection; PCR and Southern blot analysis confirmed disruption of the second copy of *INT1* in the Ura⁺ *int1/int1* homozygote (CAG3) and Ura⁻ *int1/int1* homozygote (CAG4). Northern (RNA) blot analysis confirmed that *INT1* transcript was expressed in CAI4 and CAG1 and was absent in CAG3.

14. *INT1* was reintegrated into the genome of CAG4 by transforming with a Bgl II restriction digest mixture of pDF118, which contains the *INT1* Bgl II–Sal I fragment inserted between the Bam HI and Sal I sites of pVEC (provided by P. Magee and B. Magee, University of Minnesota). The presence of *INT1* in Ura⁺ transformants was confirmed by PCR. Conventional Southern blots as well as Southern blots of chromosomes separated by pulsed-field gel electrophoresis indicated that *INT1-CaURA3* reintegrated within the *int1* locus on chromosome 5.
15. D. R. Radford, S. J. Challacombe, J. D. Walter, *J. Med. Microbiol.* **40**, 416 (1994).
16. H. Liu, J. Köhler, G. R. Fink, *Science* **266**, 1723 (1994); J. R. Köhler and G. R. Fink, *Proc. Natl. Acad. Sci. U.S.A.* **93**, 13223 (1996).
17. Induction of hyphae was tested in 20% serum added to either yeast extract–peptone-dextrose (YPD) or SD minus uracil media, in RPMI 1640 medium, and in Lee's medium and was not significantly different between CAF2, CAG1, CAG3, and CAG5 strains.
18. E. Leberer *et al.*, *Proc. Natl. Acad. Sci. U.S.A.* **93**, 13217 (1996).
19. S. M. Saporito-Irwin, C. E. Birse, P. S. Sypherd, W. A. Fonzi, *Mol. Cell. Biol.* **15**, 601 (1995).
20. M. F. Cole, W. H. Bowen, X. J. Zhao, R. L. Cihlar, *FEMS Microbiol. Lett.* **126**, 177 (1995).
21. H.-J. Lo *et al.*, *Cell* **90**, 939 (1997).
22. C. Gale and J. Berman, unpublished data.
23. W. Fonzi and M. Irwin, *Genetics* **134**, 717 (1993).
24. M. Johnston and R. Davis, *Mol. Cell. Biol.* **4**, 1440 (1984).
25. Protease-deficient *S. cerevisiae* strains YMH6 [BJ3501 (*MATα pep4::HIS3 prb1 his3-ura3 can1 gal2*) transformed with pCG01 (*3*)] and YMH7 [BJ3501 transformed with the *GAL1-10* vector pBM272 (*24*)] were grown for 8 hours at 30°C in SD minus uracil and containing 2% raffinose and 2% galactose. Cells were washed three times with 10 ml of phosphate-buffered saline (PBS) and resuspended in 400 μl of 50 mM $NaHCO_3/Na_2CO_3$ (pH 8.5) containing sulfo-NHS-LC-biotin (1 mg/ml). Cells were resuspended by vortexing for 1 s and were incubated on ice for 120 min, with periodic mixing. Cells were then incubated on ice for 1 hour with 1 ml of 100 mM tris-HCl (pH 8) to inactivate unreacted biotin. Cells were washed three times with PBS, pelleted, and resuspended in 500 μl of RIPA buffer [50 mM tris (pH 8.0), 300 mM NaCl, 1% NP-40, 0.5% deoxycholate, and 0.1% SDS] containing protease inhibitors [1 mM benzamidine, 1 mM EGTA, 1 mM EDTA, 1 mM phenylmethylsulfonyl fluoride, 1 mM 4-(2-aminoethyl)benzenesulfonyl fluoride, 0.1 mM TLCK, 0.1 mM TPCK, leupeptin (3 μg/ml), and pepstatin A (3 μg/ml)] and disrupted by vortexing for 10 min at 4°C with an equal volume of 500-μm glass beads. The resulting lysate was cleared by centrifugation at 10,000*g*, 4°C, for 30 min. Protein (9 mg) from each lysate was incubated at 0°C with 8 μg of a mixture of affinity-purified antibodies (raised in rabbits against four peptides from the translated Int1p sequence) for 60 min in a total of 800 μl of 0.33× RIPA buffer (final concentration of antibodies, 10 μg/ml). An equal amount of lysate was incubated with a 1:850 dilution of Rap1p antiserum containing ~8 μg of Rap1p antibody [S. Enomoto, P. D. McCune-Zierath, M. Gerami-Nejad, J. Berman, *Genes Dev.* **11**, 358 (1997)] under the identical conditions. An equal volume of a 10% slurry of protein A–Sepharose Fast Flow in 0.33× RIPA buffer with protease inhibitors was added to each sample and rotated for 60 min at 4°C. Samples were pelleted, and the bead pellet was washed three times with 500 μl of 0.33× RIPA buffer containing protease inhibitors. SDS-PAGE reducing buffer [20 mM tris (pH 6.8), 10% glycerol, 0.005% bromphenol blue, 2% SDS, and 5% β-mercaptoethanol; 200 μl] was added to the pellets and the samples were boiled for 5 min at 100°C. Samples were frozen at −80°C, thawed, and separated on a 7.5% SDS-PAGE gel. Proteins were transferred to a nitrocellulose membrane that was incubated either with horseradish peroxidase (HRP)–avidin (1:50,000 dilution) or with antibodies (500 ng/ml), washed, and incubated with HRP-conjugated goat antibody to rabbit IgG. Blots were developed with the Supersignal CL-HRP Substrate System.
26. [^{35}S]Methionine (specific activity, 800 Ci/mmol) was diluted to a final concentration of 8.7 μM methionine and added to exponentially growing yeast cells. Unlabeled yeast cells used to calculate nonspecific adhesion were grown identically. Yeast cells were harvested in midexponential phase, incubated for 1 hour at 37°C with monolayers of human cervical carcinoma epithelial (HeLa) cells, and washed to remove nonadherent cells before release of the monolayer for scintillation counting. Specific adhesion was calculated as the difference between total adhesion [(cpm adherent cells/cpm total cells) × 100] and nonspecific adhesion, the latter measured in the presence of a 100-fold excess of unlabeled yeast cells as described [K. S. Gustafson, G. M. Vercellotti, C. M. Bendel, M. K. Hostetter, *J. Clin. Invest.* **87**, 1896 (1991)]. For antibody blockade, yeast cells were preincubated with nonimmune rabbit IgG (1 mg/ml) or Int1p antibody UMN13 (1 mg/ml). IgG fractions of rabbit antisera or nonimmune serum were prepared by elution at pH 3.0 from a protein A matrix. Statistical significance was determined by analysis of variance followed by Fisher's protected least significant difference (StatView, version 4.51). Significance for all statistical comparisons was set at $P < 0.05$. Results are reported as specific adhesion, expressed as means ± SE ($n \geq 3$).
27. To induce hyphal growth, we grew *C. albicans* strains to stationary phase in SD minus uracil at 30°C and then inoculated them on milk-Tween agar [S. Jitsurong, S. Kiamsin, N. Pattararangrong, *Mycopathologia* **123**, 95 (1993)] or on Spider medium (*16*) with 1.35% agar, followed by incubation for 5 days at 30° and 37°C, respectively, to yield approximately 100 colonies per plate.
28. *Candida albicans* strains were cultured in SD minus uracil at 30°C. Midexponential-phase cultures were harvested, washed twice with distilled water, and diluted to a final concentration of 10^7 cells/ml. The virulence of the strains was tested in a normal mouse model system as described [J. M. Becker, L. K. Henry, W. Jiang, Y. Koltin, *Infect. Immun.* **63**, 4515 (1995)]. Male ICR mice (22 to 25 g, Harlan Sprague-Dawley) were housed five per cage; food and water were supplied ad libitum, according to NIH guidelines for the ethical treatment of animals. Mice were inoculated with 10^6 cells in a final volume of 100 μl through the lateral tail vein. The genotype of recovered isolates was verified by PCR, using primers specific for the *INT1* locus.
29. We thank B. Magee and S. Grindle for technical advice; W. Fonzi, S. Sanders, I. Herskowitz, and J. Konopka for yeast strains and plasmids; C. Asleson for technical assistance; S. Enomoto for assistance with image processing; D. Finkel for technical assistance; and P. Magee, J. Beckerman, S. Enomoto, C. Asleson, S. Johnston, B. Corner, B. Magee, and J. Lew for critical reading of the manuscript. Supported by NIH grants AI25827 and HD00850 and an endowment from the American Legion Heart Research Foundation to M.K.H., a Pediatric Scientist Development Program Fellowship to C.A.G., a Burroughs Wellcome Scholar Award to J.B., and Child Health Research Center awards (HD33692) to (C.M.B. and C.A.G.). This work is dedicated to the memory of Martin van Adelsberg.

30 September 1997; accepted 7 January 1998

Melatonin Production: Proteasomal Proteolysis in Serotonin *N*-Acetyltransferase Regulation

Jonathan A. Gastel, Patrick H. Roseboom, Peter A. Rinaldi, Joan L. Weller, David C. Klein*

The nocturnal increase in circulating melatonin in vertebrates is regulated by 10- to 100-fold increases in pineal serotonin *N*-acetyltransferase (AA-NAT) activity. Changes in the amount of AA-NAT protein were shown to parallel changes in AA-NAT activity. When neural stimulation was switched off by either light exposure or L-propranolol–induced β-adrenergic blockade, both AA-NAT activity and protein decreased rapidly. Effects of L-propranolol were blocked in vitro by dibutyryl adenosine 3′,5′-monophosphate (cAMP) or inhibitors of proteasomal proteolysis. This result indicates that adrenergic-cAMP regulation of AA-NAT is mediated by rapid reversible control of selective proteasomal proteolysis. Similar proteasome-based mechanisms may function widely as selective molecular switches in vertebrate neural systems.

An important component of vertebrate circadian and seasonal physiology is a large nocturnal increase in circulating melatonin (*1*), which results from an increase in pineal serotonin *N*-acetyltransferase (arylalkylamine *N*-acetyltransferase) (AA-NAT) activity. High nocturnal values decrease rapidly (half-life ~3.5 min) after light exposure in the middle of the night (*2*). These changes are regulated by an adrenergic-cAMP mechanism (*3*), but are otherwise poorly understood.

Section on Neuroendocrinology, Laboratory of Developmental Neurobiology, National Institute of Child Health and Human Development (NICHD), National Institutes of Health, Bethesda, MD 20892–4480, USA.

*To whom correspondence should be addressed. E-mail: klein@helix.nih.gov